JOURNAL OF MATERIALS SCIENCE 33 (1998) 405–415

ESEM observations of SCC initiation for 4340 high strength steel in distilled water

A. ATRENS
Department of Mining, Minerals and Materials Engineering, The University of Queensland, Brisbane Qld 4072, Australia

Z. F. WANG
State Key Laboratory of Corrosion Science, Institute of Corrosion and Protection of Metals, The Chinese Academy of Sciences, Shenyang 110015, People's Republic of China

The stress corrosion cracking (SCC) initiation process for 4340 high strength steel in distilled water at room temperature was studied using a new kind of instrument: an environmental scanning electron microscope (ESEM). It was found that the applied stress accelerated oxide film formation which has an important influence on the subsequent SCC initiation. SCC was observed to initiate in the following circumstances: (1) cracking of a thick oxide film leading to SCC initiation along metal grain boundaries, (2) the initiation of pits initiating SCC in the metal and (3) SCC initiating from the edge of the specimen.

All these three SCC initiation circumstances are consistent with the following model which couples SCC initiation with cracking of a surface protective oxide. There is a dynamic interaction between oxide formation, the applied stress, oxide cracking, pitting and the initiation of SCC. An aspect of the dynamic interaction is cracks forming in a protective surface oxide because of the applied stress, exposing to the water bare metal at the oxide crack tip, and oxidation of the bare metal causing crack healing. Oxide crack healing would be competing with the initiation of intergranular SCC if an oxide crack meets the metal surface at a grain boundary. If the intergranular SCC penetration is sufficiently fast along the metal grain boundary, then the crack yaws open preventing healing of the oxide crack. If intergranular SCC penetration is not sufficiently fast, then the oxidation process could produce sufficient oxide to fill both the stress corrosion crack and the oxide crack; in this case there would be initiation of SCC but only limited propagation of SCC. Stress-induced cracks in very thin oxide can induce pits which initiate SCC, and under some conditions such stress induced cracks in a thin oxide can directly initiate SCC.

1. Introduction

Stress corrosion cracking (SCC) [1] is a complex process which involves the combination of mechanical, physical and chemical processes that accomplish the separation of bonds at the initiation site or at the crack tip, thereby initiating or advancing the SCC crack. A vast amount of effort has been expended over the last fifty years on trying to understand SCC initiation in terms of pitting [2, 3], anodic dissolution [4, 5], film rupture [6, 7] or hydrogen embrittlement [8, 9]. Furthermore, different mechanisms control SCC for different material–environment combinations. For example, SCC for pipeline steels in a carbonate–bicarbonate solution at -600 mV (standard calomel electrode; SCE) is associated with anodic dissolution after surface film rupture [10]; whilst SCC of 4340 high strength steel in water is thought to be controlled by hydrogen embrittlement [11–13].

SCC [1] often occurs under corrosive conditions where general corrosion is not a problem. The corrosion resistance of interest is caused by surface films that separate the material from its environment. Such films can cause a low rate of general corrosion despite a large thermodynamic driving force for corrosion. For example, stainless steels are stainless because of a very thin passive surface layer which is essentially Cr_2O_3. Although this layer is so thin (typically less than 4 nm [14–17]) that it cannot be seen with the naked eye, this layer is nevertheless effective in separating the steel from its environment. The passive films on stainless steels are usually self repairing. The breakdown of such films can be induced chemically (e.g. by chlorides), and pitting corrosion results when the breakdown is localized. Localized film breakdown under the joint action of a stress and an environment is the essence of SCC. Cracking of surface films has been shown to be involved for SCC initiation in pipeline steels [18, 19] and high strength steels [20–22].

Our prior work has dealt extensively with SCC of steels. A new test method for SCC was developed

[23, 24]: the linearly increasing stress test (LIST) and was applied to high strength steels [23, 24], pipeline steels [10], carbon steel [25] and pure copper [26]. Stress rate effects have been shown [18–26] to be an important part of the SCC mechanism, and in particular crack tip creep has been shown to be an important part of the SCC mechanism for high strength steels undergoing SCC in water [18–27], which can provide [27] an explanation for the stationary cracks observed in service. Room temperature creep has been measured for high strength steels including AISI 4340 and AerMet100 [28] and related to crack initiation [21]. A new model was proposed for SCC for quenched and tempered steels based on strain assisted dissolution [29]. Stress corrosion crack velocity was measured [30] and was related to heat treatment and microstructure [31, 32]. The possible causes for the intergranular crack path for high strength steels undergoing SCC in water have been explored by microstructural characterization using electron microscopy [33–35], measurements of grain boundary chemistry [36] and electrochemistry [37]. A precipitation strengthened duplex stainless steel was developed [38].

The development and application of micromeasurement technology is required to advance our knowledge of the processes occurring during SCC initiation. Detailed observations and measurements are needed down to the atomic level to understand the issues involved including for example the chemical influence on bond breaking. A possible step in the direction of appropriate micromeasurement technology may be provided by the environmental scanning electron microscope (ESEM).

The ESEM [39] differs from a conventional scanning electron microscope (SEM) by allowing the direct imaging of physical and biological materials in their natural state. Specimen temperature, moisture content and gas environment can be manipulated whilst continuously observing the specimen thus allowing direct imaging and recording of dynamic processes such as wetting, drying, absorption, corrosion, melting, crystallization and fracture. A conventional SEM requires high vacuum to operate. This means that specimens need to be dry before introduction into the SEM, and in any case the high vacuum in the SEM dries any residual moisture in the specimen. Thus, it is usually not possible to observe directly a metallic specimen in contact with liquid water as occurs in the SCC process. There are several low vacuum SEMs and environmental stages, but none offer the high pressure capabilities of the ESEM [39].

The ESEM overcomes the limitations of the high vacuum of SEMs by permitting the entire specimen chamber to be held at a much higher pressure (up to 2.6 MPa). Simultaneously, a high vacuum is maintained in the electron gun and electron column areas by means of clever design and differential pumping of the various regions of the ESEM.

The ESEM is a recently developed instrument. It allows *in situ* high magnification viewing of a specimen while it is stressed and simultaneously subjected to a controlled aqueous environment. ESEM has been used in a preliminary study to explore the crack tip strain for 4340 [1, 40, 41]. Our recent work [19] evaluated the use of ESEM in the study of SCC initiation for X52 steel in a carbonate–bicarbonate solution. This indicated that SCC initiation involved the formation and cracking of a surface oxide film. However, this work highlighted the limitation of the ESEM in such research in that SCC of pipeline steels in carbonate–bicarbonate solutions is a relatively slow process, even though this is a typical SCC system [42, 43]. This limitation might be overcome by the study of a model system where the SCC processes are much faster such as 4340 high strength steel in water in which case there are high SCC velocities in the range 1×10^{-4} to 1×10^{-7} m s^{-1} [1, 12, 13, 44] and that is the purpose of the work reported in this paper.

This paper presents detailed ESEM observations of SCC initiation for 4340 high strength steel in distilled water. Possible SCC initiation mechanisms are proposed.

2. Experimental procedure

The material was 4340 high strength steel with chemical composition as shown in Table I. A flat tapered specimen shape was used, as illustrated in Fig. 1. To prevent distortion, all specimens were held by a jig during heat treatment: austenitized 2 h at 860 °C in high-purity argon and oil quenched. The yield strength was 1270 MPa. After heat treatment, the specimen gauge sections were polished with 800 grit emery paper.

The loading stage is shown in Fig. 2; this could be installed and moved freely in the ESEM chamber. Calibration of the stage indicated that the load on the specimen F_s (in N) was given by

$$F_s = 57.45d + 1.9 \quad (1)$$

where d(mm) was the crosshead displacement and was related to the displacement of the springs. (This measure of d has been adopted for experimental

TABLE I Chemical composition (wt %) of 4340 steel

C	Cr	Ni	Mn	Mo	P	S	Si	V
0.36	1.64	1.50	0.6	0.25	0.01	0.005	0.30	0.06

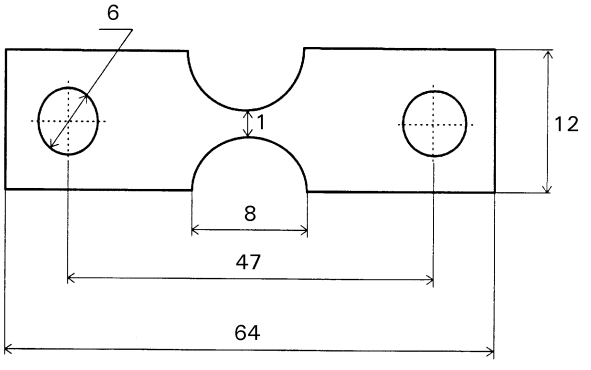

Figure 1 Specimen configuration. Dimensions in mm. Thickness = 1 mm.

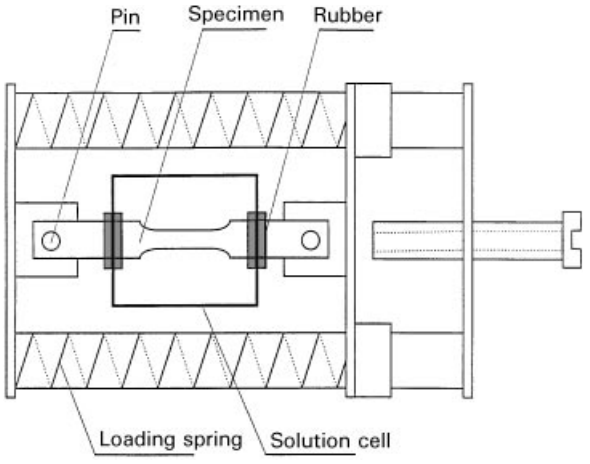

Figure 2 Schematic top view of the loading stage.

convenience. Equation 1 gives $F_s = 1.9$ N when $d = 0$, because for this value of d, there is already some spring compression. Thus it is emphasized that d is a measure of crosshead displacement and is linearly related to spring compression.) Thus, there was a linear relationship between the applied load on the specimen and spring displacement. This loading stage and choice of specimen shape allowed a constant load to be applied to each specimen with the result that there was a range of stress values along the specimen; the stress values decreased with distance along the specimen from the maximum stress at the minimum section. In the SCC experiments reported in this paper, each specimen was subjected to a tension stress of 1450 to 1500 MPa at the narrowest part.

Prior to testing, each specimen was cleaned using alcohol and distilled water, and the specimen was immediately mounted into the loading stage. The distilled water was poured into the cell to cover the specimen surface and simultaneously the tensile stress was applied. All experiments were carried out in an aerated distilled water at room temperature at the free corrosion potential.

During the SCC experiments, the specimen surface was covered by the water. Unfortunately, ESEM observations of the specimen surface are not possible through a water layer, (because the electrons of the primary beam would be all absorbed in such a layer). To enable ESEM observation of the specimen surface, the water level was lowered below the specimen, causing an interruption of the SCC exposure.

Such observations were carried out after total exposure times of 1, 4, 12, 15, 24 and 48 h, as summarized in Table II.

The results for specimen A are recorded in Figs 3, 4, 7, 8 and 9. Specimen A was exposed to distilled water for 1 hour under stress, the distilled water was removed and ESEM observations (Fig. 3) were carried out of specimen A under load by introducing specimen A fully loaded in the loading stage into the ESEM apparatus. The ESEM observations were carried out at a partial pressure of typically 359–532 Pa. This prevented full drying out of the surface oxide film which could be an important consideration for the subsequent re-initiation of SCC. The ESEM observations took about half an hour after which the SCC exposure was restarted by pouring fresh distilled water into the solution cell. ESEM observations of specimen A were carried out for a second time (Fig. 4) after a further 3 h exposure to distilled water under stress which corresponds to a total exposure time of 4 h. Similarly ESEM observations of specimen A were carried out for a third time (Figs 7–9) after a further 11 h exposure to distilled water under stress, which corresponds to a total exposure time of 15 h.

Specimen B was exposed to distilled water for 12 h, after which specimen B was unloaded and examined in the ESEM (Fig. 5) to determine if unloading prior to examination caused any discernible difference. The results were similar as will be seen from a comparison of Figs 4 and 5. Subsequently specimen B was reloaded in distilled water and broke completely into two parts after 5 days.

Specimen C broke after 2 h of exposure to distilled water under load before any surface observations were undertaken.

Specimen D was exposed to distilled water for 24 h under load, unloaded for ESEM observation (Fig. 10), exposed to distilled water for a further 24 h under load (48 h total exposure time), unloaded for ESEM observations (Fig. 11), and subsequently specimen D broke completely when reloaded in distilled water. The SCC fracture surface is typical and is shown in Fig. 6.

Specimen E was used to investigate the direct influence of the SCC solution on the specimen with no applied load. Specimen F explored the influence of the

TABLE II Specimen details

Specimen	Total exposure time, t_{ex} (h)	Specimen loaded during ESEM examination	Fig. no.	Time to failure, *ttf* (h)
A	1	yes	3	
A	4	yes	4	
A	15	yes	7, 8, 9	> 15 h
B	12	no	5	5 days
C	2 → break	–	–	2 h
D	24	no	10	
D	48	no	11	
D	load → break	no	6	48 h
E	no load	no	12	
F	24 with load			
F	24 with no load			

SCC solution (distilled water) on the specimen under conditions of no load after first exposure under load.

3. Results

Fig. 3 shows the specimen surface appearance for specimen A after 1 h of exposure at stress to distilled water. It could be seen with the naked eye that rust (brown in colour) covered some parts of the surface. After the rust was removed by light brushing, an oxide film (dark in colour) could be seen on the specimen surface; this is illustrated in Fig. 3a where the parts appearing like a shadow correspond to this dark oxide film. Fig. 3b, a typical higher magnification view of the "shadow" area of Fig. 3a, shows two different areas: in the middle of the field of view is an area continuously covered with an oxide of significant thickness which has many fine cracks as shown in even greater detail in Fig. 3c; the rest of the field of view of Fig. 3b corresponded to an oxide-covered surface with the oxide thickness being small except for numerous mounds, blacker in contrast, of greater thickness. Fig. 3c shows that there were many fine cracks in the continuous oxide film. These small cracks did not seem to be related to metal grain boundaries because the size of these cracks was smaller than the grain size. There were also pits on the oxide film, as illustrated in Fig. 3d, but no SCC initiation was caused by these pits.

ESEM observations of specimen A were carried out for a second time (Fig. 4) after a futher 3 h exposure to distilled water under stress which corresponds to a total exposure time of 4 h. Fig. 4a shows an ESEM view of the brown rust covering the surface. This was very loose and was easily removed by brushing. After the brown rust was removed the dark oxide film with cracks was visible, Fig. 4b.

Specimen B (4340 continuously exposed for 12 h to distilled water at stress) gave a similar result, as shown by a comparison of Fig. 5 and Fig. 4b. The size and morphology of these oxide cracks was very similar to the grain size as observed on a typical SCC fracture surface, as shown in Fig. 6 for specimen D. The SCC fracture surface showed totally intergranular SCC cracking as expected for SCC of high strength steels in water. This provided a strong indication that the oxide cracks shown in Figs 4 and 5 were probably initiating SCC and furthermore, the oxide film that caused the SCC initiation was thick compared to the oxide film covering other areas of the surface. Note that the oxide crack morphology shown in Figs 4 and 5 typical after exposure for 4 and 12 h to distilled water under

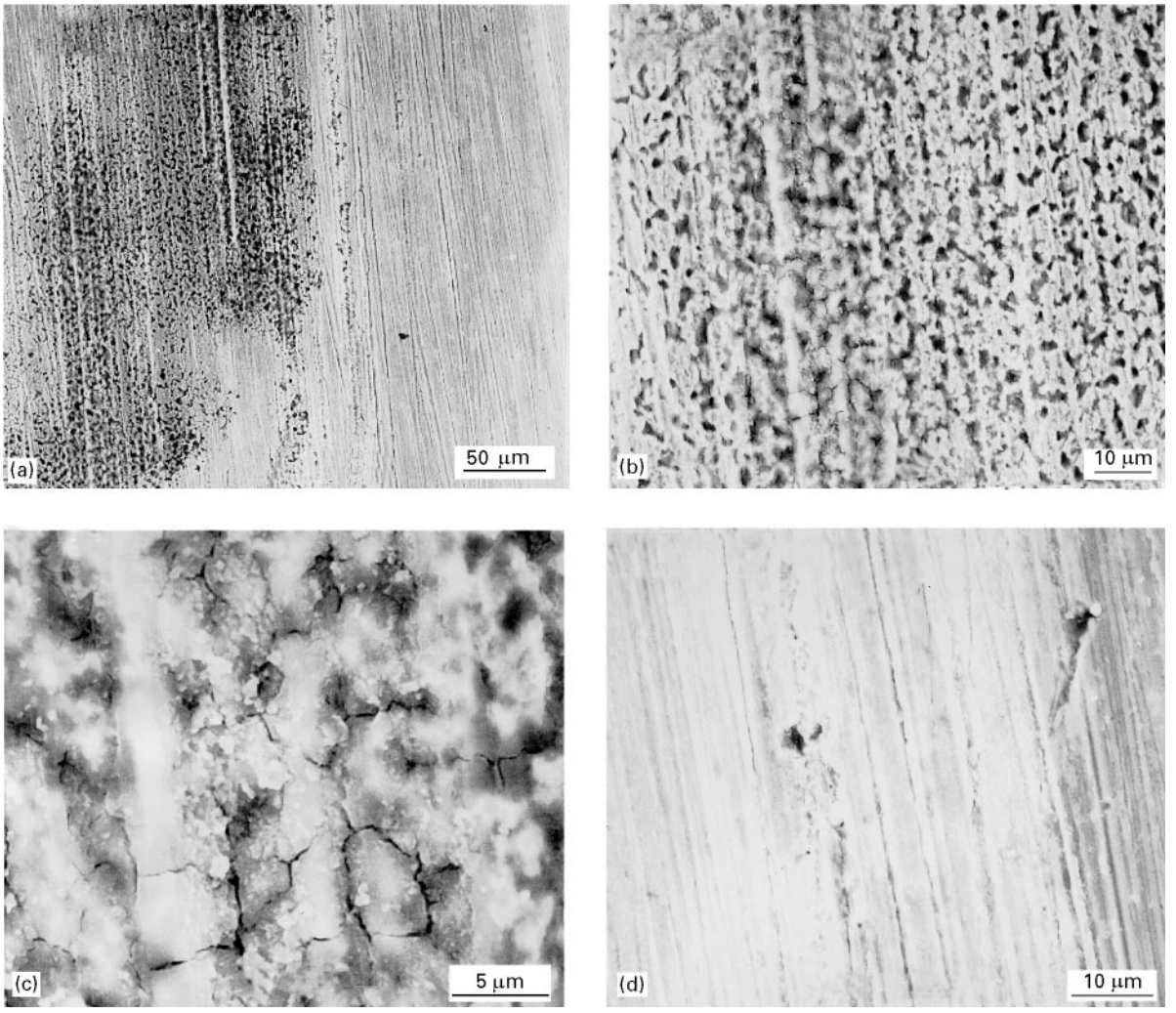

Figure 3 Surface appearance after 1 h exposure, specimen A: (a) oxide film at low magnification, (b) and (c) oxide film at higher magnification and (d) pits.

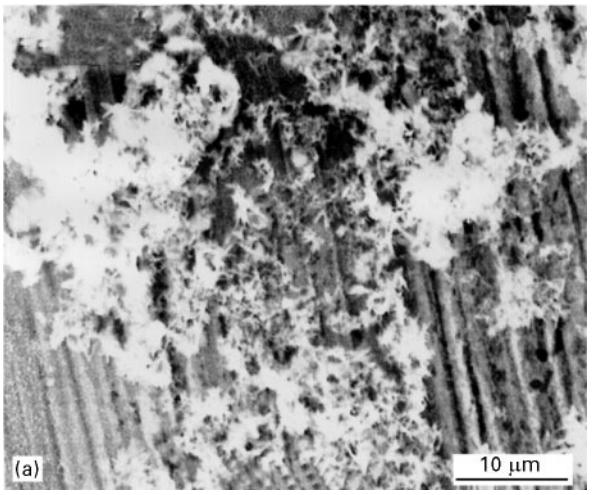

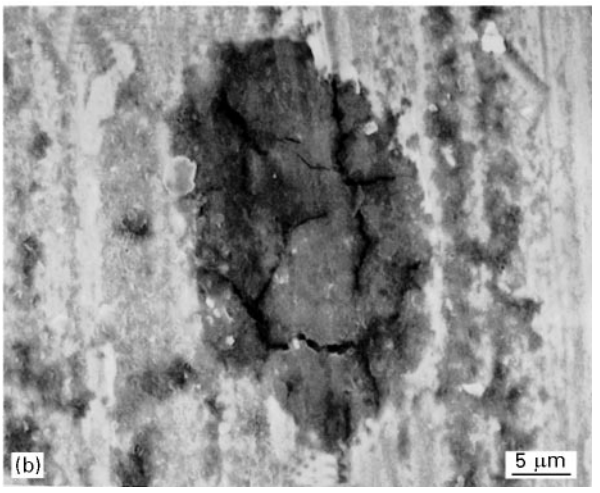

Figure 4 Oxide film appearance on specimen A after a total of 4 h exposure to water at stress.

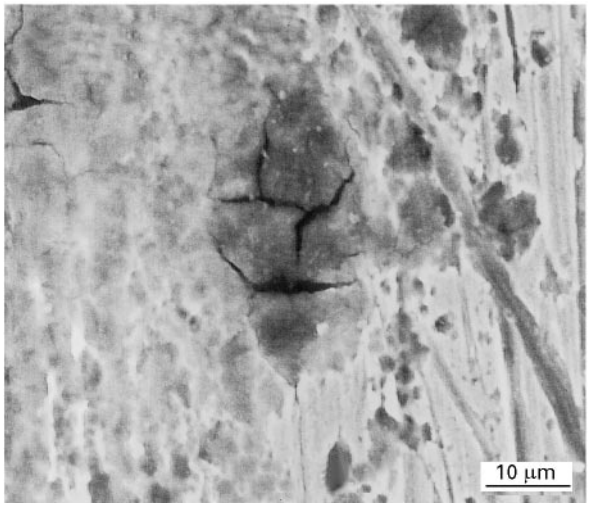

Figure 5 Oxide film appearance on the surface of specimen B after 12 h exposure to distilled water at stress.

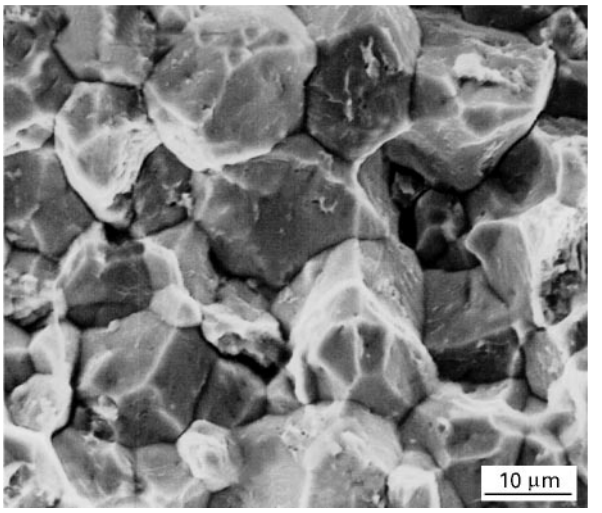

Figure 6 Typical intergranular SCC fracture surface, specimen D.

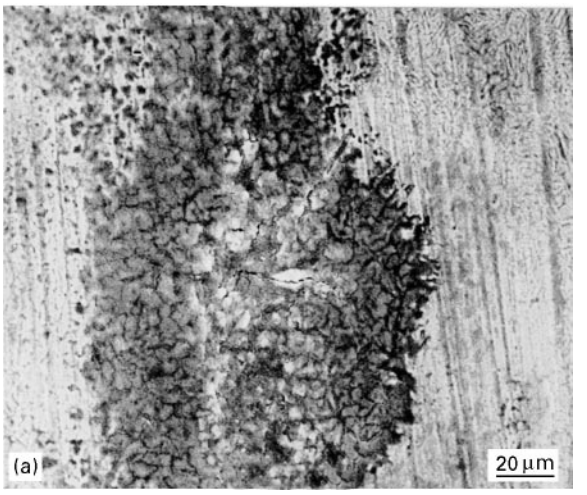

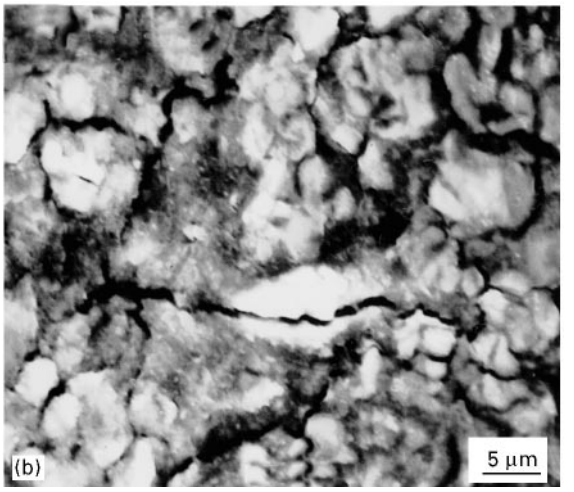

Figure 7 Oxide film appearance for specimen A after a total exposure time of 15 h to distilled water under load.

stress respectively is significantly different to the oxide crack morphology, as illustrated in Fig. 3c typical for 1 h exposure to distilled water under stress. This leads to the issue of how the oxide cracks observed after 1 h exposure to water under stress could transform to give a crack morphology similar to that of the grain boundaries as observed for the oxide cracks after longer exposure to distilled water under stress.

ESEM observations of specimen A were carried out for a third time after a further 11 h exposure to distilled water under stress which corresponds to a total exposure time of 15 h, Figs 7, 8 and 9. All the specimen

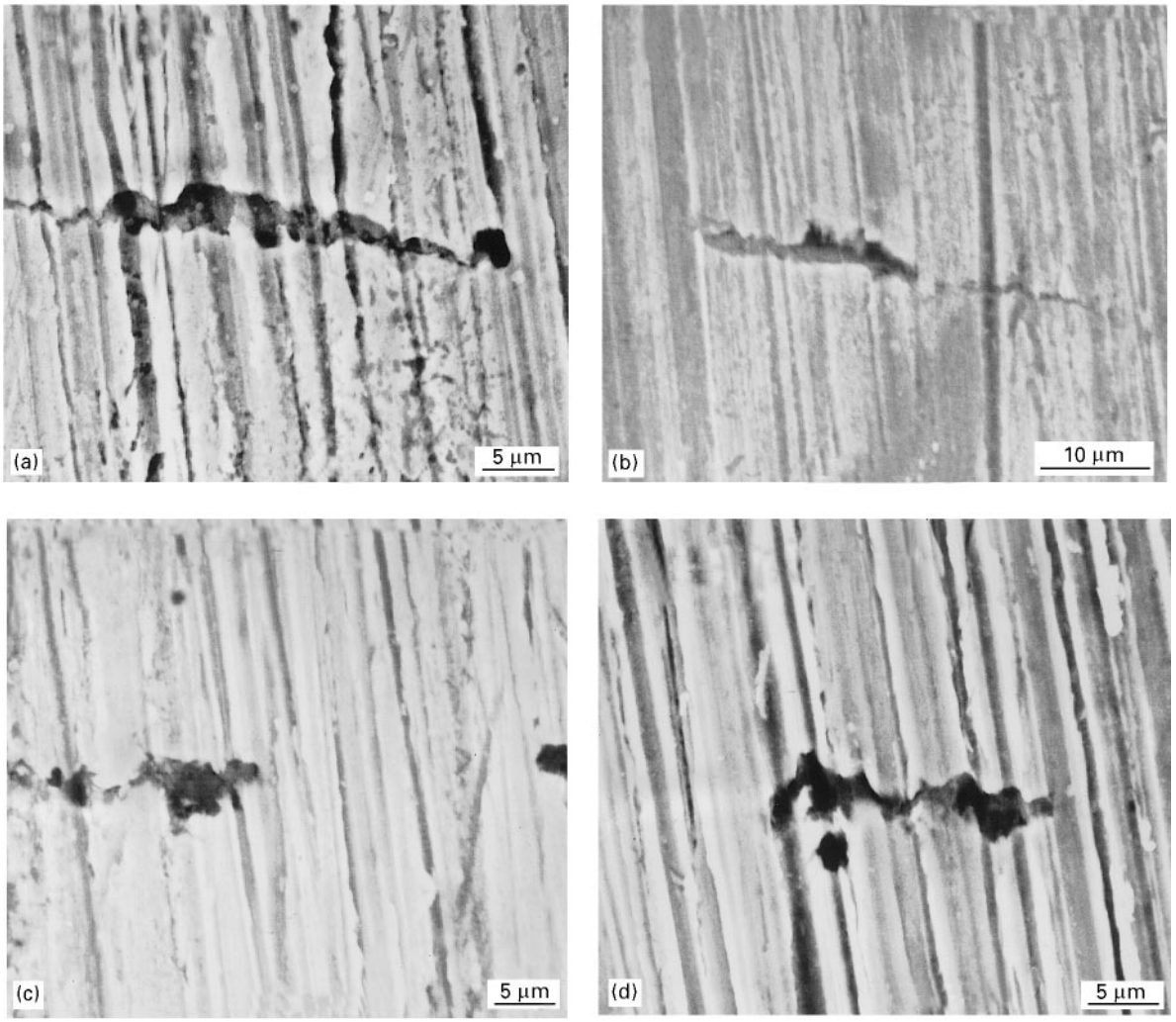

Figure 8 In areas of thin oxide for specimen A after a total exposure of 15 h to distilled water at stress it was common for a line of pits to initiate with the line perpendicular to the tensile direction, and for these pits to initiate SCC which linked the pits.

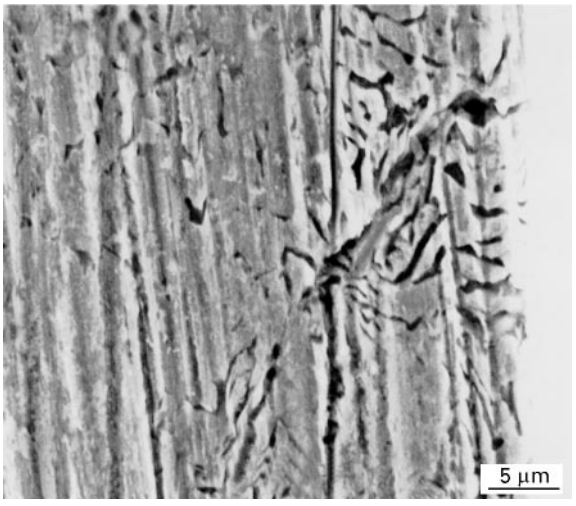

Figure 9 SCC initiation at the edge for specimen A after a total exposure of 15 h to distilled water at stress.

surface was covered by an oxide film at this time as illustrated in Fig. 7a although the oxide thickness varied from place to place. In some sites, the thick oxide film had flaked off. In areas where there was thick oxide, the cracks in the oxide were large, and the crack shape and size was related to the grain size and morphology, as shown in Fig. 7b which is a higher magnification view of Fig. 7a. These cracks had become large and connected with each other perpendicular to the loading direction which was vertical for this figure. It is thought that there were many small cracks and that some of these had linked together perpendicular to the direction of the maximum tensile stress and thereby had become quite long in this direction. Fig. 8 illustrates that in areas of thin oxide it was common for a line of pits to initiate in a line perpendicular to the tensile direction, and for these pits to initiate SCC which linked the pits. Fig. 8a shows a case where SCC has joined at least four distinct pits. Similarly, three and five pits are linked in Fig. 8b and d, respectively. Fig. 8c shows an intermediate case where the two pits on the left of the field of view are connected by SCC whereas the pit on the right is still isolated; it is expected that the SCC will in time also connect to this pit. Fig. 9 shows SCC initiation at the edge of the specimen. Both the pits and the specimen edge are sites with a high stress concentration where SCC was observed to initiate easily.

Fig. 10 shows the appearance of the specimens surface for specimen D after continuous exposure of 24 h

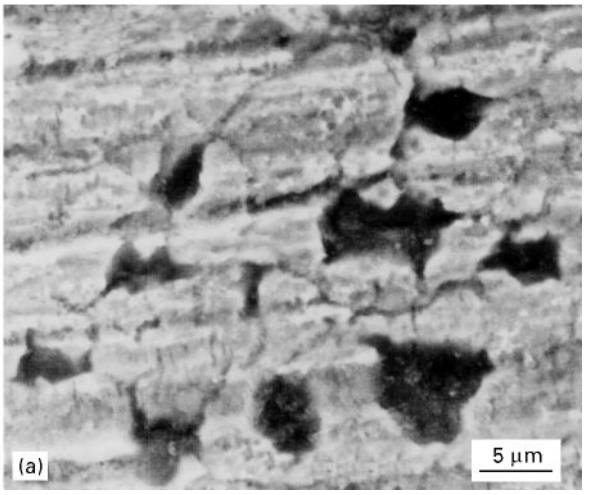

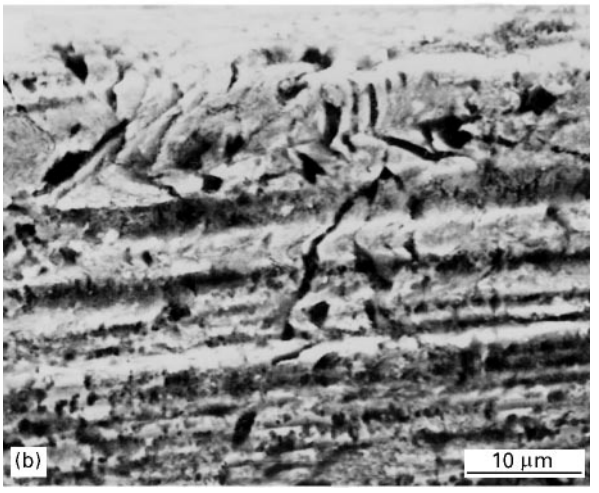

Figure 10 Surface appearance of specimen D after exposure of 24 h to water at load: (a) middle part and (b) the edge of the specimen.

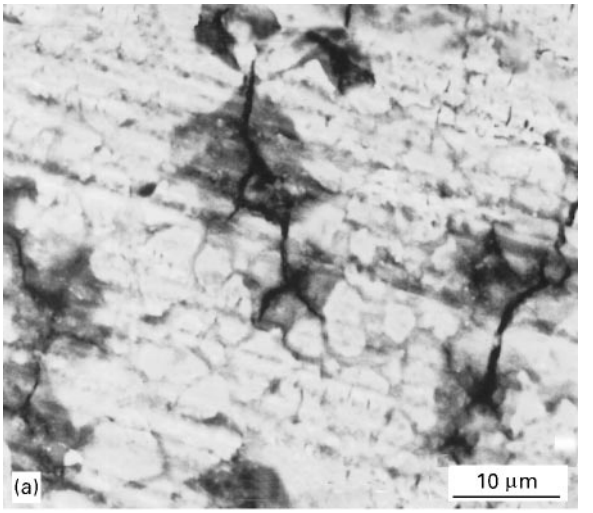

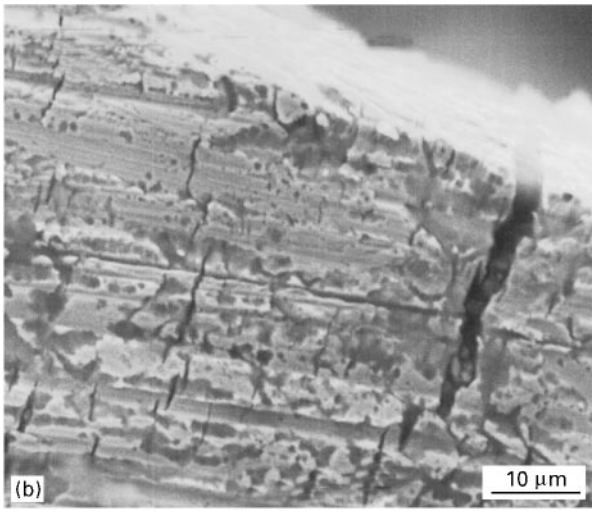

Figure 11 Surface appearance of specimen D after a total exposure time of 48 h to water at stress: (a) middle part and (b) the edge of the specimen.

to water at stress. The SCC initiation was easily found at the edge (Fig. 10b) and the middle part (Fig. 10a) of the specimen. In the middle part of the specimen, the SCC cracks were initiated at the bottom of the pits and then connected each other. Many pits formed at this time. Unlike pipeline steel in carbonate–bicarbonate solution [18, 19], most pits caused SCC initiation.

Fig. 11 shows the appearance of the specimen surface for specimen D after a total exposure time of 48 h in water, indicating nearly the same results as with 24 h exposure. The SCC cracks had become larger and had connected each other.

Specimen E was exposed to water with no applied stress to observe the oxide film formation characteristics. Oxide film formation with no applied stress was more difficult than under conditions of applied stress. There was no observable change on the specimen surface for up to 6 h of exposure to water. After 24 h of exposure to water a few parts of the specimen surface were covered with an oxide film. Fig. 12a shows the appearance of the oxide film on the specimen surface after exposure of 24 h to water with no applied stress. At some sites, the oxide film was thick and at the other sites, the oxide film was thin, whilst on most parts of the specimen, there was no visible oxide film. Fig. 12b shows cracks in the thick oxide film. These cracks were similar to those shown in Fig. 3b and c. Fig. 12c shows that there were fewer cracks in the thin oxide film; however, there were many pits in the area with the very thin oxide film, as shown in Fig. 12d.

Furthermore, specimen F was exposed to distilled water for 24 h at stress. After the rust was removed from the surface, specimen F was exposed to water again this time without any applied stress. Oxide film formation was not as easy as for this same specimen with no applied stress as with an applied stress. These observations indicated that the applied stress was involved in the formation of the oxide film on the specimen surface.

4. Discussion

Table II summarizes the specimen details. A particularly noteworthy feature is the large variation in the time to failure for identical experiments: from 2 h to 5 days which represents a variation by a factor of 60. As-quenched 4340 high strength steel is very susceptible to SCC with reported crack velocities in the range 10^{-4} to $10^{-7}\,\mathrm{m\,s^{-1}}$. With $v = 10^{-4}\,\mathrm{m\,s^{-1}}$, the

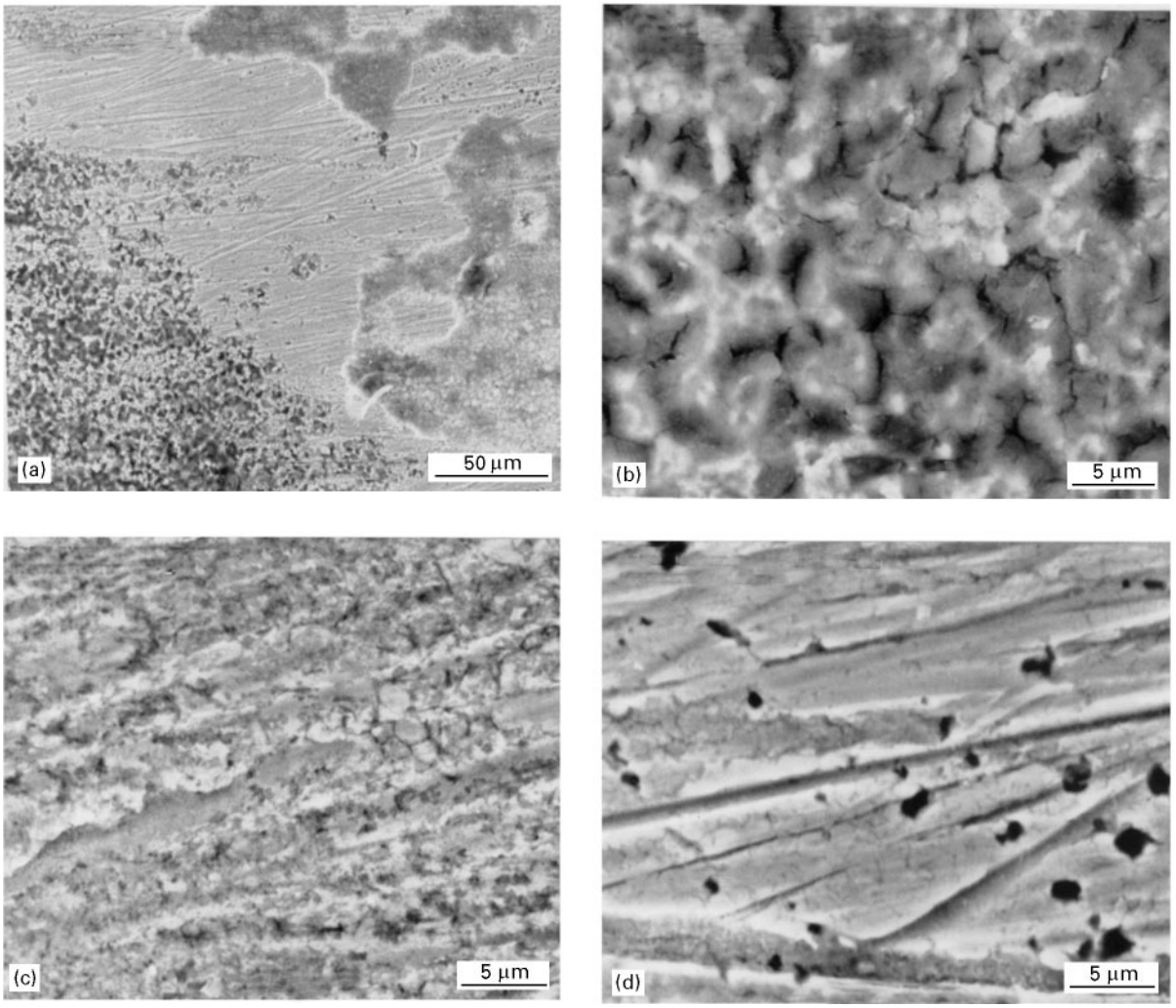

Figure 12 Surface appearance after 24 h exposure at no applied stress: (a) oxide film at low magnification; (b) thick oxide film with cracks; (c) thin oxide film with less cracks; and (d) pits formation on the thin oxide film.

1 mm specimen section would be penetrated in 10 s, whereas with $v = 10^{-7}\,\mathrm{m\,s^{-1}}$, the specimen lifetime would correspond to 3 h after SCC initiation. This indicates that 3 h at most would be taken up with SCC propagation, and that any period greater than about 3 h must be associated with SCC initiation. Thus most of the variation in time to failure is probably associated with the initiation of SCC.

The oxide film started to form on the specimen surface soon after the specimen was exposed to water at an applied stress. At the beginning, the oxide film occurred at a few sites. More oxide grew on the specimen surface with increasing time until it covered all specimen surface. In places where the oxide was thick, oxide film was obviously in two layers, with brown rust on top of a blacker oxide. The rust layer was very easily removed by brushing, and thus was very lightly bound to the substrate. It is expected that this brown rust had no influence on SCC initiation which was associated with the more adherent oxide which was black in colour when it was of sufficient thickness.

The oxide film became thicker with increasing time. However, the thickness of the oxide film was different at different sites. Unlike the oxide film for pipeline steel in carbonate–bicarbonate solution, which was mainly associated with the applied potential and less with applied stress [18], the oxide film for 4340 high strength steel in water at the free corrosion potential was mostly associated with applied stress as is clear from a comparison of experiments exposing at 4340 specimens to distilled water with and without load.

The oxide film is a necessary part of the process in the initiation of SCC cracks. Fig. 13 summarizes the observations for 4340 high strength steel in distilled water. Three initiation circumstances were observed: (1) thick oxide film cracking leading to SCC in the metal, (2) the initiation of pits initiating SCC in the metal and (3) SCC initiating from the edge of the specimen. For the first case, the cracks in the thick oxide film easily initiated SCC cracks due to the high stress concentration and appropriate chemistry inside the cracks. However, the fracture surface appearance, as shown in Fig. 6, indicated an intergranular path for SCC propagation in this system. Figs 4 and 5 also show that SCC initiated intergranularly. These observations indicated that only the large oxide cracks with the appropriate orientation, for example, perpendicular to the applied stress direction, are favoured to initiate SCC cracks. The result in Fig. 7b and Fig. 8 supported this conclusion. The pits and the edge of the specimen are stress concentration sites where it was usually easy to initiate SCC.

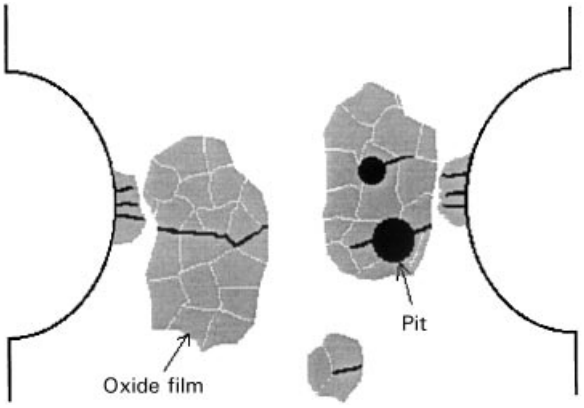

Figure 13 Three circumstances for the initiation of SCC.

Note that the oxide crack morphology shown in Figs 4 and 5 was typical after exposure for 4 and 12 h to distilled water under stress, respectively, was significantly different to the oxide crack morphology, as illustrated in Fig. 3c, typical for 1 h exposure to distilled water under stress. This leads to the issue of how the oxide cracks observed after 1 h exposure to water under stress could transform to give a crack morphology similar to that of the grain boundaries as observed for the oxide cracks after longer exposure to distilled water under stress as typified by Figs 4 and 5. There are two possibilities that relate to when the oxide cracks form: (1) while the oxide is in the water under stress or (2) when the oxide starts to dry out.

The first possibility is that the cracks in the oxide form while the oxide is immersed in the distilled water. Oxide cracks were observed experimentally to form preferentially at metal grain boundaries for specimens exposed to the water for times longer than one hour. Such oxide cracks could be imagined to concentrate appropriate conditions onto the metal surface to easily initiate SCC in the underlying metal at the grain boundaries. It is also possible that such cracks would preferentially initiate grain boundary SCC in the metal only when there was a coincidence between an oxide crack and a metal grain boundary. If such a crack was not appropriately located to initiate SCC in an underlying grain boundary, then it would be expected for such an oxide crack to heal as part of the continuing oxidation of the metal surface, as oxide formation would be expected to be particularly fast at an existing oxide crack due to the easy access of the solution to bare metal. Thus oxide cracks could be in a continuous state of formation and repair with only those corresponding to metal grain boundaries remaining after significant exposure times when SCC had initiated in the grain boundaries below the oxide cracks. In this view there is a direct interaction of SCC initiation in the metal which would cause a yawing open of the oxide crack and thereby prevent sufficient oxidation of the metal (which would cause the crack to heal). This provides a dynamic model of oxide cracks forming due to the applied stress, exposing to the water bare metal at the oxide crack tip, and oxidation of the bare metal causing crack healing. Oxide crack healing would be competing with the initiation of intergranular SCC if the oxide cracks meet the metal surface at a grain boundary. If intergranular SCC penetration is sufficiently fast along the metal grain boundaries, then the crack yaws open preventing healing of the oxide crack. If intergranular SCC penetration is not sufficiently fast, then the oxidation process could produce sufficient oxide to fill both the stress corrosion crack and the oxide crack; in this case there would be initiation of SCC but only limited propagation of SCC. Such SCC initiation and limited propagation is a common observation [42, 43] in pipeline steels and could correlate in the above mechanism with a slow crack propagation velocity.

The second possibility to explain the difference in crack morphology between Fig. 3c and Fig. 4 is the possibility that the oxide protects the underlying metal from corrosion whilst the oxide is in the distilled water, but cracks form in the oxide when the oxide is subjected to drying conditions as occurs for example when the sample is taken out of the distilled water for observation. Such oxide cracks would nevertheless be expected to contain some water or moisture. Cracking of the oxide would therefore bring water into direct contact with the metal thereby bringing about conditions at the metal surface appropriate to the initiation of SCC. The oxide crack morphology could be related to the oxide thickness and to the distribution of deformation within the metal grains.

The present research does not provide any experimental observations to allow unambiguous differentiation between these two possibilities and this is clearly an interesting avenue for further research. Both possibilities have merit. The second possibility could help to explain the very large spread in the time to failure 2 h to 5 days observed in the present research for identical experiments. However, the first possibility has considerable support from the observations that stress accelerates the oxide film formation. A strong possibility for the mechanism by which stress could accelerate oxide film formation is a mechanism of oxide cracking exposing bare metal to corrosion/oxidation by the distilled water. Further strong support for an applied stress causing oxide film cracking comes from the observation of stress-induced pitting and the linking of such pits by stress corrosion cracks oriented perpendicular to the direction of maximum tensile stress, as shown in Fig. 8. There does not seem to be any other reason why pits should become oriented with respect to the tensile stress; these results argue that the tensile stress has a major role in pit initiation by local oxide cracking.

Similarly, in this emerging model, stress would be involved in the initiation of SCC at the specimen edge because the edge is a stress concentrator. The mechanism would be oxide cracking caused by the stress concentration at the specimen edge. This mechanism is proposed on the basis that there would be a thin oxide covering all the specimen surface even in places where this oxide is not sufficiently thick to be obvious.

ESEM is a totally new type of instrument which has the potential to allow the *in situ* observation of SCC

initiation. However, the inherent nature of the ESEM places some limitations on its usefulness in the study of the SCC initiation.

One fundamental limitation of the ESEM is that no imaging is possible through a solution layer because such a solution layer would absorb all the electrons in the incident beam. This limitation was overcome in the present study by interrupting the SCC exposures for ESEM observation. There are questions concerning the influence of this interruption and exhaustion of creep on subsequent SCC processes. One such consequence is the drying of the oxide films; the use of the ESEM counteracts the consequences of such oxide drying as much as is possible because of the presence of water vapour in the ESEM specimen chamber during ESEM observation.

It could be beneficial to use ESEM for studying SCC initiation in gaseous environments, for example, titanium and its alloys in hydrogen gas. The process of formation of hydrides induced by applied stress will be easily observed.

5. Conclusions

An applied stress was found to accelerate the formation of oxide film on the specimen. Many small cracks observed on the thick oxide film. Pits were formed on the thin oxide film. SCC was observed to initiate in the following circumstances: (1) thick oxide film cracking leading to intergranular SCC in the metal, (2) the initiation of pits initiating SCC in the metal and (3) SCC initiating from the edge of the specimen.

All these three initiation circumstances are consistent with the following model which couples SCC initiation with cracking of a surface protective oxide. There is oxide formation on the metal surface. There is a dynamic interaction between oxide formation, the applied stress, oxide cracking, pitting and the initiation of SCC. An aspect of the dynamic interaction is cracks forming in a protective surface oxide due to the applied stress, exposing to the water bare metal at the oxide crack tip, and oxidation of the bare metal causing crack healing. Oxide crack healing would be competing with the initiation of intergranular SCC if the oxide cracks meet the metal surface at a grain boundary. If intergranular SCC penetration is sufficiently fast along the metal grain boundaries, then the crack yaws open preventing healing of the oxide crack. If intergranular SCC penetration is not sufficiently fast, then the oxidation process could produce sufficient oxide to fill both the stress corrosion crack and the oxide crack; in this case there would be initiation of SCC but only limited propagation of SCC. Stress-induced cracks in very thin oxide can induce pits which initiate SCC, and under some conditions such stress-induced cracks in thin oxide can directly initiate SCC.

Acknowledgements

This work was supported by East Australia Pipeline Ltd. The authors thank PhD student N. Kinaev for his design of loading stage and heat treatment of specimens.

References

1. A. ATRENS and Z. F. WANG, *Mater. Forum* **19** (1995) 9.
2. T. K. CHRISTMAN, *Mater. Perf.* **30** (1991) 23.
3. *Idem. Corrosion* **46** (1990) 450.
4. R. N. PARKINS, in "Fundamental aspects of SCC", edited by R. W. Staehle, A. J. Forty and D. V. Rooyen (Houston, TX, NACE, 1969) p. 361.
5. P. R. RHODES, *Corrosion* **25** (1969) 462.
6. A. J. McEVILY, A. P. BOND, *J. Electrochem. Soc.* **112** (1965) 112.
7. E. N. PUGH, in "The theory of SCC in alloys", edited by J. C. Scully (NATO, Brussels, 1977) p. 21.
8. A. R. TROIONO, "Hydrogen in Metals", edited by I. M. Berstein, (Met. Soc. AIME, 1974) p. 12.
9. P. R. RHODES, *Corrosion* **25** (1969) 462.
10. Z. F. WANG and A. ATRENS, *Metall. and Mater. Trans.* **27A** (1996) 2686.
11. S. RAMAMURTHY and A. ATRENS, *Corrosion Sci.* **34** (1993) 1385.
12. M. O. SPEIDEL, in "Corrosion in power generating equipment", M. O. Speidel and A. Atrens (Plenum, Oxford and hb 1984) p. 85.
13. R. MAGDOWSKI PEDRAZZOLI and M. O. SPEIDEL, in "Parkins Symposium on fundamental aspects of stress corrosion cracking", edited by S. M. Bruemmer, E. I. Meletis, R. H. Jones, W. W. Gerberich, F. P. Ford and R. W. Staehle (TMS, Warrendale, Pennsylvania 1992) 341.
14. S. JIN and A. ATRENS, *Appl. Phys. A* **42** (1987) 149.
15. *Idem., ibid.* **50** (1990) 287.
16. A. S. LIM and A. ATRENS, *ibid.* **53** (1992) 273.
17. *Idem., ibid.* **54** (1992) 500.
18. Z. F. WANG and A. ATRENS, *J. Mater. Sci.* Accepted for publication.
19. *Idem., ibid. J. Mater. Sci.*
20. A. ATRENS, Z. F. WANG, N. KINAEV, D. R. COUSENS and J. Q. WANG, in Proceedings of 13 International Corrosion Congress, Melbourne (1996).
21. A. OEHLERT and A. ATRENS, *Mater. Forum* **17** (1993) 415.
22. *Idem. Corrosion Sci.* **38** (1996) 1159.
23. A. ATRENS, C. C. BROSNAN, S. RAMAMURTHY, A. OEHLERT and I. O. SMITH, *Measurement Sci. Technol.* **4** (1993) 1281.
24. S. RAMAMURTHY and A. ATRENS, *Corrosion Sci.* **34** (1993) 1385.
25. A. ATRENS and A. OEHLERT, *J. Mater. Sci.* submitted.
26. J. SALMOND and A. ATRENS, *Scripta Metall. Mater.* **26** (1992) 1447.
27. R. M. RIECK, A. ATRENS and I. O. SMITH, *Met. Trans.* **20A** (1989) 889.
28. A. OEHLERT and A. ATRENS, Overview No 114 *Acta Metall. Mater.* **42** (1994) 1493.
29. A. ATRENS, R. M. REICK and I. O. SMITH, in "ICF7 Advances in Fracture Research, edited by K. Salama, K. Ravi-Chandar, D. M. R. Taplin and P. Rama Rao (Pergamon Press, Oxford, 1989) p. 1603.
30. A. OEHLERT and A. ATRENS, *J. Mater. Sci.* **32** (1977) in press.
31. R. M. RIECK, A. ATRENS and I. O. SMITH, *Mater. Forum.* **13** (1989) 48.
32. *Idem., ibid.* **13** (1989) 54.
33. J. D. GATES, A. ATRENS and I. O. SMITH, *Z. fur Werkstofftechnik* **18** (1987) 165.
34. *Idem., ibid* **18** (1987) 179.
35. *Idem., ibid* **18** (1987) 344.
36. J. SKOGSMO and A. ATRENS, *Acta Metall. Mater.* **42** (1994) 1139.
37. S. RAMAMURTHY, A. ATRENS, I. O. SMITH, *Mater. Sci. Forum* **44 & 45** (1989) 139.
38. A. ATRENS, R. COADE, J. ALLISON, H. KOHL, G. HOCHERTLER and G. KRIST, *Mater. Forum* **17** (1993) 263.
39. P. J. R. UWINS, *ibid.* **18** (1994) 51.

40. N. N. KINAEV, A. ATRENS, D. R. COUSENS and R. MILLER, in Proceedings of 14th Australian Conference on Electron Microscopy, Sydney (1996) A95.
41. A. ATRENS, Z. F. WANG, N. KINAEV, D. R. COUSENS and J. Q. WANG, in Proceedings of 13 International Corrosion Congress, Nov 1996, Melbourne.
42. R. N. PARKINS, E. BELHIMER and W. K. BLANCHARD Jr, *Corrosion* **49** (1993) 951.
43. R. N. PARKINS, W. K. BLANCHARD Jr, B. S. DELANTY, *ibid*. **50** (1994) 395.
44. H. R. BAKER, C. R. SINGLETERRY, *ibid*. **28** (1972) 340.

Received 23 July 1996
and accepted 24 July 1997